Nontraditional (Per)oxy Ring-Closure Paths in the Atmospheric Oxidation of Isoprene and Monoterpenes

Luc Vereecken* and Jozef Peeters

Department of Chemistry, University of Leuven, Celestijnenlaan 200F, B-3001 Heverlee, Belgium

Received: February 20, 2004; In Final Form: April 13, 2004

In the atmospheric oxidation of organic compounds, free peroxy and oxy radicals play a crucial role. The traditional view is that peroxy radicals react with NO or with other (hydro-)peroxy radicals, whereas oxy radicals decompose, undergo a hydrogen shift, or react with O_2. However, we show in this quantum chemical and statistical-rate investigation that the presence of a double C═C bond in many (per)oxy radicals formed from isoprene and monoterpenes, the most abundant nonmethane hydrocarbons emitted into the atmosphere, can result in hitherto neglected ring-closure isomerizations. These processes are shown to be competitive under atmospheric conditions and can substantially alter the predicted oxidation products. As an illustration, the major pathways in the OH-initiated oxidation of β-pinene are discussed. It is shown that the predominance of the (per)oxy ring-closure routes offers a consistent rationalization for the "anomalously" low observed yields of traditional-pathway oxidation products from this compound.

I. Introduction

The biogenic hydrocarbons isoprene (2-Me-1,3-butadiene) and the monoterpenes ($C_{10}H_{16}$ compounds such as α-pinene, β-pinene, *d*-limonene, phellandrene, myrcene, etc.; see Figure 1 for some example structures) constitute ca. 50% of the global mass of volatile organic compounds (VOCs) released into our atmosphere.[1] In their main source areas (i.e., tropical and boreal forests), they dominate the tropospheric VOC-oxidation chemistry, whereas on a global scale, they strongly influence the tropospheric free-radical and ozone budgets and hence the atmospheric oxidizing capacity.[2,3] Moreover, they are the main precursors of secondary organic aerosols (SOA), which affect the radiative budget directly and indirectly.[4,5] Although their main oxidation pathways have been unraveled thanks to numerous experimental and theoretical investigations (see, for example, refs 6−15), some 30−40% of the oxidation product mass from isoprene and an even larger product fraction from the major monoterpenes still await quantification. The accuracy of air-quality models depends on a complete understanding of the oxidation mechanisms of these ubiquitous VOCs.

The atmospheric oxidation of these VOCs is initiated largely by OH addition to a double bond, resulting in β-hydroxy-alk-(en)yl radicals R• (Scheme 1) and subsequently in organic peroxy radicals ROO• via fast reaction with O_2. At NO levels ≥100 pptv as in polluted areas, the ROO• are thought to react predominantly with NO, forming organic alk(en)oxy radicals, RO•, and NO_2. Fast photolysis of NO_2 regenerates NO and yields O atoms that combine rapidly with O_2 to produce ozone. At lower NO levels, ROO• reactions with HO_2 and R′O_2 radicals lead to hydroperoxides, oxy radicals, and carbonyl and/or hydroxy compounds. For organic oxy radicals, RO•, as formed in the reactions described above, three subsequent pathways are generally accepted (Scheme 1): decomposition, isomerization by a hydrogen shift, and H abstraction by O_2.[16] The rate of the unimolecular reactions (decomposition and isomerization) is highly dependent on the exact structure of the oxy radical examined.

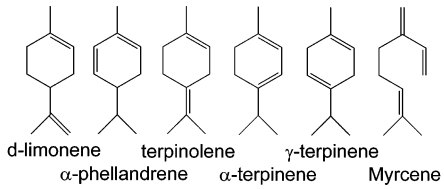

Figure 1. Some typical monoterpenes that lead to unsaturated peroxy radicals after reaction with OH and O_2. The most abundant monoterpenes, α-pinene and β-pinene, are shown in Scheme 3.

SCHEME 1: Traditional Reactions of Peroxy and Oxy Radicals Formed in the Atmospheric Degradation of Volatile Organic Compounds (VOCs)

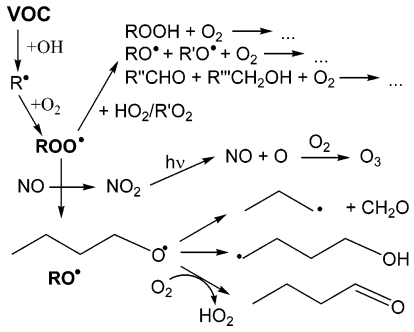

For isoprene and the terpenes, however, the traditional (per)-oxy radical reactions outlined above may be insufficient to describe the degradation chemistry and to predict oxidation products because many of the resulting ROO• and RO• radicals are unsaturated and may undergo hitherto neglected ring-closure reactions as their dominant atmospheric fate. An example of such a ring-closure reaction is shown in Scheme 2 for the template 3-buten-1-peroxy radical. These types of ring-closure reactions have escaped observation thus far. This need not

* Corresponding author. E-mail: luc.vereecken@chem.kuleuven.ac.be.

10.1021/jp049219g CCC: $27.50
Published on Web 05/25/2004

SCHEME 2: Ring Closure in the Template CH_2═CH−CH_2−CH_2OO• Peroxy Radical, Followed by Fast Reaction with O_2[a]

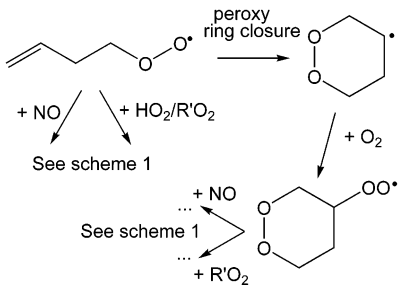

[a] The cyclic peroxide-ring peroxy radical is expected to react according to the traditional reactions shown in Scheme 1.

surprise us because in laboratory experiments the NO or HO_2/R′O_2 radical concentrations are generally much higher[6−14] than atmospheric values, such that their bimolecular reactions with the ROO• at issue can easily outrun the unimolecular ring-closure reaction. The scarcely available "low-NO_x" experiments with low HO_2/R′O_2 concentrations[12−14] focused on a limited number of specific products and/or total yields of the major generic classes of products (aldehydes, carbonyls, etc.) or quantified only a limited fraction of the product mass.

In this work, we describe the results of a theoretical study of the ring-closure reactions of unsaturated peroxy- and oxy radicals as formed in the atmospheric oxidation of isoprene and terpenes. The absolute rate coefficient for ring closure is calculated by transition-state theory (TST) based on a detailed quantum chemical analysis of the reactants and transition states and is compared to the rate of competing reactions to assess their importance at atmospheric conditions. Because there is virtually no data available on these types of unimolecular ring-closure reactions, we will first establish the reliability of our quantum chemical methodology by examining a number of reference reactions and template molecules. The TST calculations include tunneling effects and explicitly incorporate the temperature-dependent population of *all* of the rotamers of the reactants and transition states (TSs). The precise mathematical implementation of these multirotamer TST calculations is described elsewhere;[17] its application improves the prediction of the temperature dependence of the rate coefficient by an explicit incorporation of the different orientations of the internal rotors and a rigorous accounting of the changes in the number of internal rotors and their characteristics. These effects tend to be important, particularly in ring-closure and -opening reactions because a significant number of internal degrees of freedom of rotation are lost or gained.

II. Methodology

We selected the B3LYP-DFT[18,19] method (geometries and rovibrational data using the 6-31G(d_{5d},p) basis set with five spherical d functions (5d), combined with single-point energy calculations using the 6-311+G(2d,p) basis set) for the quantum chemical characterization of the reactants and transition states: this method is sufficiently fast to allow extended calculations on the large monoterpene molecules while still yielding reliable relative energies and rovibrational data. To verify the reliability of the B3LYP-DFT method specifically for peroxy- and oxy-radical ring closures, we performed some targeted calculations on reference molecules. To our knowledge, there are no studies on unimolecular unsaturated-peroxy ring-closure reactions except for the highly specific case of aromatics,[20−22] though numerous data are available for the bimolecular counterparts.[23] From these latter data, we selected the *i*-C_3H_7OO• + propene reaction as a reference reaction. We also performed a detailed theoretical analysis of the CH_2═CH−CH_2−CH_2OO• radical, the simplest template molecule for peroxy-radical ring closure forming a six-membered peroxide ring structure. Because virtually no experimental data seem to be available for the addition of oxy radicals to double bonds, bimolecular or unimolecular, we compare theoretical results at different levels of theory for the CH_3O + C_3H_6 reaction as a test for oxy-radical ring closure.

The first verification of the methodology involves the bimolecular *i*-C_3H_7OO• + propene reaction, for which an activation energy E_A of 16.2 ± 0.6 kcal mol^{-1} was determined experimentally;[23] the quoted uncertainty is the stated experimental error. B3LYP-DFT/6-311+G(2d,p) energy calculations on B3LYP-DFT/6-31G(d,p) optimized geometries yielded a barrier height E_b of 15.9 kcal mol^{-1}, which is very close to the experimental E_A value. Note that basis sets that are too small yield significant basis set superposition errors for bimolecular reactions and should not be used. Full optimizations using the 6-311+G(2d,p) and 6-311++G(2df,2pd) basis sets resulted in barrier heights of 15.9 and 16.1 kcal mol^{-1}, respectively. We did not perform a TST analysis on this reaction to account for the difference between barrier height E_b and Arrhenius activation energy E_A because these kinetic calculations are rather sensitive to the (often poor) description of the low-frequency bending/tumbling modes in the TS of this type of bimolecular reaction. The equivalent unimolecular reactions, the subject of this paper, have ring-shaped TSs and are much less sensitive to this problem. Nonetheless, even without an explicit theoretical calculation of E_A, it is clear that the barrier height E_b calculated with B3LYP-DFT is fully compatible with the experimental data, indicating that this methodology is capable of properly describing this type of reaction.

As a second test, we compare B3LYP-DFT results against high-level CCSD(T) calculations for the CH_2═CH−CH_2−CH_2-OO• peroxy radical, a simple template molecule subject to the peroxy-radical ring closure (Scheme 2). The CCSD(T) method is computationally too expensive for use on larger molecules but is well established as a method that gives barrier heights and reaction enthalpies of high reliability. Table 1 summarizes the relative energies calculated at several levels of theory. The 27 different rotamers for the CH_2═CH−CH_2−CH_2OO• radical are labeled by the attitude of dihedral angles between the C═C−C−C, C−C−C−O, and C−C−O−O atoms. (See the caption of Table 1 for details.) Four ring-closure TSs were found, resulting in a six-membered peroxide ring, two enantiomers with a chair configuration, and two enantiomers in the boat form. Only the chair-form peroxide-ring reaction product was found to be stable; the boat form converges to the chair form without an apparent barrier. All levels of theory used agree on the barrier height, $E_{ringclose}$ = 17.6 ± 0.4 kcal mol^{-1}. The energy spacing between the different rotamers is also consistent over all levels of theory used, though the cost of the CCSD(T) calculations prohibited a full investigation of this aspect. We additionally investigated the use of ultrafine DFT integration grids but found no significant effect for any of the rotamers or TSs. Note that the formation of a five-membered peroxide ring faces a much higher barrier because of ring strain (e.g., $E_{ringclose}$ = 30 kcal mol^{-1} for the CH_2═CH−CH_2OO• peroxy radical) and is of no importance. The only significant difference found between B3LYP and CCSD(T) is the relative energy of the closed peroxide ring, with a systematic difference of

TABLE 1: Relative Energies Relevant to the Ring Closure in the CH_2═$CH-CH_2-CH_2OO^{\bullet}$ Radical, Including 27 Reactant Rotamers, 2 Ring-Closure Transition Structures, the Peroxy Ring Structure, and Rearrangement to an Epoxide−Alkoxy Structure from This Peroxy Ring Structure

level of theory: geometry:	B3LYP-DFT/6-31G(d,p)		B3LYP-DFT/6-311+G(2d,p)	
energy:	B3LYP-DFT[a]	CCSD(T)[a]	B3LYP-DFT[a]	CCSD(T)[a]
rotamer[b] (enantiomer)[c]	E_{rel} (kcal mol^{-1})	E_{rel} (kcal mol^{-1})	E_{rel} (kcal mol^{-1})	E_{rel} (kcal mol^{-1})
CH_2═$CH-CH_2-CH_2OO^{\bullet}$ ctt	1.0	1.0	1.1	1.1
CH_2═$CH-CH_2-CH_2OO^{\bullet}$ cpt (cmt)	1.3		1.4	
CH_2═$CH-CH_2-CH_2OO^{\bullet}$ ctp (ctm)	1.0		1.0	
CH_2═$CH-CH_2-CH_2OO^{\bullet}$ cpp (cmm)	1.4		1.4	
CH_2═$CH-CH_2-CH_2OO^{\bullet}$ cpm (cmp)	1.4		1.4	
CH_2═$CH-CH_2-CH_2OO^{\bullet}$ ptt (mtt)	0.2		0.2	
CH_2═$CH-CH_2-CH_2OO^{\bullet}$ ppt (mmt)	0.3		0.4	
CH_2═$CH-CH_2-CH_2OO^{\bullet}$ ptp (mtm)	0.2		0.2	
CH_2═$CH-CH_2-CH_2OO^{\bullet}$ pmt (mpt)	0.6		0.6	
CH_2═$CH-CH_2-CH_2OO^{\bullet}$ ptm (mtp)	**0.0**	**0.0**	**0.0**	**0.0**
CH_2═$CH-CH_2-CH_2OO^{\bullet}$ ppp (mmm)	0.3		0.3	
CH_2═$CH-CH_2-CH_2OO^{\bullet}$ ppm (mmp)	0.9		0.9	
CH_2═$CH-CH_2-CH_2OO^{\bullet}$ pmp (mpm)	1.00		0.9	
CH_2═$CH-CH_2-CH_2OO^{\bullet}$ pmm (mpp)	0.5		0.5	
TS ring-closure chair	17.2	17.9	17.2	17.9
TS ring-closure boat	22.3	23.5	22.4	23.4
peroxy ring chair	4.8	2.6	4.9	2.5
TS to epoxide−alkoxy	26.4		26.2	

[a] (Single-point) energy calculations using the 6-311+G(2d,p) basis set. [b] Rotamer names CH_2═$CH-CH_2-CH_2OO^{\bullet}$ xyz are based on the main dihedral angles of the internal rotors. x denotes the C═C−C−C angle (c = cis, for dihedral angles close to 0°; p = plus, for angles close to +120°; and m = minus, for angles close to −120°); y denotes the C−C−C−O angle (t = trans, for angles close to 180°; p = plus, about +60°; and m = minus, about −60°); and z denotes the C−C−O−O dihedral angle (same notation as for the C−C−C−O angle). See Supporting Information for Cartesian coordinates. [c] The enantiomer (designation given in parentheses) has all dihedral angles reversed in sign but has identical energetic and rovibrational properties.

TABLE 2: Barrier Heights for the Addition of CH_3O Radicals to C_2H_4, Calculated at Various Levels of Theory

level of theory: geometry:	B3LYP-DFT/6-31G(d,p)		B3LYP-DFT/6-311+G(2d,p)		B3LYP-DFT
energy:	B3LYP[a]	CCSD(T)[a]	B3LYP[a]	CCSD(T)[a]	6-311++G(2df,2pd)
rotamer (enantiomer)	E_{rel} (kcal mol^{-1})	E_{rel} (kcal mol^{-1})	E_{rel} (kcal mol^{-1})	E_{rel} (kcal mol^{-1})	E_{rel} (kcal mol^{-1})
$CH_3O + C_2H_4$	0.0	0.0	0.0	0.0	0.00
TS addition	5.7	7.0	6.1	7.4	6.3

[a] (Single-point) energy calculations using the 6-311+G(2d,p) basis set.

∼2.3 kcal mol^{-1} (Table 1). To determine the impact of this uncertainty on kinetic predictions, it is instructive to perform a TST analysis of the ring-closure and ring-reopening rate coefficients, incorporating the temperature-dependent population over all rotamers and TSs. The rate for ring closure is found to be $k_{ringclose} = 1.4 \times 10^{-2}$ s^{-1} at 298 K, which is comparable to the combined rates of the reactions with NO and HO_2/R′O_2 at typical levels of these species in pristine environments (i.e., ∼(1−3) × 10^{-2} s^{-1}).[16,24−25] The ring-reopening rate coefficient is predicted to be 2.5 × 10^3 s^{-1} using the B3LYP reaction endoergicity of 4.9 kcal/mol (i.e., the value that favors ring opening most). Using the CCSD(T) value of 2.5 kcal mol^{-1} yields a ring-reopening rate that is ∼50 times slower. Under atmospheric conditions, this ring reopening must compete with the fast recombination reaction of the cyclic radical with O_2 (Scheme 2), with a pseudofirst-order rate coefficient of roughly ∼5 × 10^7 s^{-1}.[16] Obviously, ring reopening cannot be competitive with the O_2 reaction; in fact, even when both methods seriously underpredict the relative energy of the cyclic product radical by 3 kcal/mol, ring reopening remains negligibly slow (<1%) compared to reaction with O_2, making the current uncertainty of the reaction endoergicity a void issue. This remains true for the other ring-reopening reactions studied in this paper. Bimolecular reactions of peroxy radicals with olefins are typically followed by rearrangement to an epoxide + alkoxy structure. For the cyclic peroxides at issue, the ring structure hampers this rearrangement, resulting in very high barriers (Table 1). Thus, epoxide−alkoxy formation is not a viable competitive channel for the compounds studied in this work.

Barrier heights calculated for the $CH_3O + C_3H_4$ addition reaction using various quantum chemical methods are shown in Table 2. In contrast to the peroxy-radical reactions, we find that B3LYP-DFT underestimates the addition barrier systematically by about 1.3 kcal mol^{-1} compared to the predictions made using high-level CCSD(T) theory. Preliminary calculations on the unimolecular ring closure in pentenoxy radicals also show a similar underestimation of the barrier height. This issue will be investigated in more detail in future work. For the time being, a kinetic comparison with other competing reactions will have to account for a possible underestimation of the DFT barrier by 1 to 3 kcal mol^{-1} compared to the predicition of CCSD(T). The geometry optimized at the 6-31G(d,p) basis set is of lower quality because of basis set superposition errors, causing the single-point calculations on this geometry to be somewhat lower than the other results; this effect will have a negligible influence on our calculations on unimolecular reactions of larger hydrocarbons.

The results detailed above all indicate that the B3LYP-DFT level of theory is capable of describing the reactions of peroxy radicals featuring C═C bonds, yielding results that compare favorably with experiment and high-level quantum chemical methods. In particular, B3LYP-DFT/6-311+G(2d,p) single-point

SCHEME 3: OH-Initiated Formation of Peroxy Radicals for Isoprene, α-Pinene, and *β*-Pinene, Followed by Peroxy Ring Closure and Reaction with O_2 Leading to Cycloperoxide−Peroxy Radicals, Which Are Expected to React According to the Traditional Peroxy Radical Paths Given in Scheme 1

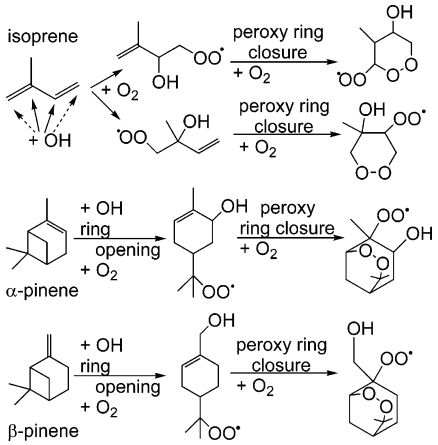

energies on B3LYP-DFT/6-31G(d,p) geometries seem to be within 1 kcal/mol of more advanced CCSD(T) methods, at a very reasonable computational cost. Therefore, we confidently select this methodology for use in the extended kinetic studies below, which can involve more than 150 rotamers per analysis for the monoterpenes. For the reactions of oxy radicals containing double bonds, there seems to be a systematic underestimation of the barrier, which will have to be accounted for.

All quantum chemical calculations were performed using the Gaussian 98 quantum chemical program.[26]

III. Peroxy Ring Closure in Isoprene

Isoprene, the most important atmospheric nonmethane VOC by far, is emitted predominantly in tropical forests at an average temperature approaching 30 °C and at typical NO, HO_2, and $R'O_2$ levels of 50, ≤30, and ≤35 pptv, respectively.[5,24−25] In the OH-initiated oxidation of isoprene, the OH radical can add onto four different C atoms (Scheme 3), followed by reaction with O_2 to form *β*-hydroxy-peroxy radicals. Addition to the two central carbons allows the subsequent formation of a six-membered peroxide ring. It is currently not yet clear which fraction of the isoprene reacts by addition on these central carbons:[6,11,27] the most detailed product distribution study to date by Warneck et al.[11] found ∼16%, but Paulson and Seinfeld[6] suggested about 40%. Theoretical predictions[28,29] tend to be lower, with our own structure−activity relationship[28] predicting about 10%. Also, about half of the initial central hydroxy-isoprene adducts are predicted to isomerize promptly prior to reaction with O_2.[30] As such, it is difficult to predict the exact fraction of isoprene that leads to the *β*-hydroxy-peroxy radicals of interest in this work. However, given the ∼600 Tg/year of isoprene globally emitted,[1] even 5% amounts to a sizable quantity.

For each of the *β*-hydroxy-peroxy radicals shown in Scheme 3, we examined the ring-closure reaction by characterizing 81 reactant conformers, cyclizing through 12 TS conformers with calculated barrier heights of 16.2 to 22.0 kcal mol^{-1} (Supporting Information). The barrier height for the formation of a tertiary radical, 16.2 kcal mol^{-1}, is about 1 kcal mol^{-1} lower than for the formation of a secondary radical, 17.0 kcal mol^{-1}, in agreement with established relative stabilities of substituted radicals and the calculations for the 1-butylperoxy radical.

Using our B3LYP-DFT quantum chemical energy, geometry, and rovibrational data, we applied statistical kinetic transition-state theory (TST) to obtain absolute rate coefficients. These calculations include tunneling effects and explicitly incorporate the temperature-dependent population of all of the rotamers of reactants and transition states.[17] The TST rate coefficient is predicted to be $k_{ringclose} \approx 0.3$ s^{-1} at 303 K. At typical laboratory NO levels of 1 to 10 ppmv, the rate of reaction with NO is 10^2-10^3 s^{-1},[16] which is much faster than our ring-closure prediction. "Low-NO_x" experiments were either performed at elevated HO_2 and $R'O_2$ levels exceeding 5 ppbv each,[11] such that $k_{HO_2/R'O_2} \approx 2$ s^{-1} outruns the ∼0.2 s^{-1} ring closure at 298 K, or quantified only a limited number of specific products and/or total yields of major generic classes of products,[13,14] such that the (reduced) fraction of ring-closure products is masked in the plethora of (unspeciated) carbonyl, (di-)hydroxy, and hydroperoxide compounds. However, our $k_{ringclose}$ result predicts that at the NO and $HO_2/R'O_2$ levels above pristine forests, the major source areas of isoprene, more than 90% of the peroxy radicals discussed will undergo ring closure. Even in moderately polluted areas, with 1 ppbv NO, the rates of ring closure and reaction with NO are still comparable. Once the peroxy ring is closed, the dominant reaction will be combination with O_2 (Scheme 2), with a rate of $\sim 5 \times 10^7$ s^{-1}.[16] Ring reopening, with a TST rate ≤10^5 s^{-1} even when accounting for possible errors of 3 kcal mol^{-1} on the relative energy of the product, and rearrangement and opening to an epoxy-oxy structure, with energy barriers of ≥20 kcal mol^{-1} due to increased ring strain, are not competitive and will not affect the chemistry. The peroxide-ring−peroxy-radical ROO• that is formed will then follow the traditional reactions of Scheme 1. For the fraction of the initial isoprene peroxy radical that reacts with NO and is converted to an alkoxy radical, ring-closure reactions are not possible in the subsequent degradation process: the B3LYP-DFT barrier to ring closure for the alkoxy radical is >15 kcal mol^{-1}, which is too high to compete with the facile *β*-hydroxy-alkoxy decomposition process. The total degradation mechanism and ultimate reaction products, depending on NO and $HO_2/R'O_2$ levels, are beyond the scope of this article.

IV. Peroxy Ring Closure in Monoterpenes

Most of the monoterpenes (see Figure 1 for some examples) have multiple double bonds, and peroxy ring-closure reactions are therefore potentially important. The most abundant terpenes, α-pinene and *β*-pinene, have only one double bond, but it has been shown that the four-membered ring is easily broken in one of the chemically activated initial OH-adduct radicals,[15,31] leading to a new double bond (Scheme 3). For α-pinene, following O_2 addition and reaction with NO, this is the dominant formation route[15,31] of acetone, an important oxygenated VOC that is a major photolytic source of HO_x in the upper troposphere[32] and a precursor to PAN, an NO_x reservoir in the atmosphere. Because the resulting peroxy radical from α-pinene already contains a six-membered ring, we must explicitly account for the relative positioning of the diverse substituents on this ring; in particular, the −OH substituent can be on the same side (syn) or the other side (anti) of the ring relative to the −OO• substituent. For each of these cases, we characterized 54 conformers and 3 ring-closure transition states. See Supporting Information for more information on these conformers. In the ROO• radical formed from α-pinene when the OH is in the syn position with the peroxy group (estimated to be about 40% of the ROO• radicals[15]), a hydrogen bond between the −OH group adjacent to the double bond and the peroxy radical

site substantially lowers $E_{ringclose}$ to ~13.8 kcal mol^{-1}. This lowering of the barrier height enhances the peroxy ring-closure rate, $k(T) = 4.77 \times 10^9 \exp(-12.6 \text{ kcal mol}^{-1}/RT)$ s^{-1}, to 2.6 s^{-1} at 298 K, which is well above the rate of the NO reaction even at 1 ppbv NO ($k_{NO} \approx 0.1$ s^{-1}) and the rates of reaction with HO_2/R′O_2 at atmospheric concentrations. Obviously, the formation of a peroxide ring changes the subsequent chemistry substantially, possibly reducing the formation of acetone but very likely promoting SOA formation in the atmosphere because another O_2 will now add (Scheme 3) and because higher degrees of oxygenation of organic compounds result in lower volatilities. With the OH group in the anti position (~60% of the population[15]) H bonding is not possible, such that the barrier to ring closure, 15.9 kcal mol^{-1}, is more comparable to that found in isoprene. The ring-closure rate, $k(T) = 4.81 \times 10^{10} \exp(-14.8 \text{ kcal mol}^{-1}/RT)$ s^{-1}, calculated to be $k_{ringclose} \approx 0.6$ s^{-1} for 298 K, is slightly faster than in isoprene and is still a dominant process at NO concentrations of 1 ppbv. We also investigated the formation of seven-membered peroxide rings, but such ring closure is too slow to be competitive: the transition states are 4−6 kcal mol^{-1} higher than those forming six-membered peroxide rings, and ring-closure rates are on the order of 10^{-4} s^{-1} or less. Additionally, we optimized the transition state for epoxide−alkoxy formation from the six-membered peroxide rings and for the analogous attack of the second oxygen atom of the peroxide function on the radical site leading to a six-membered ether ring. Both of these reactions have barriers in excess of 25 kcal mol^{-1} and will not influence the kinetics.

In the case of the major OH adduct for β-pinene (Scheme 3), the −OH group is located in the exocyclic $-CH_2OH$ rotor, allowing H-bond-assisted ring closure in all cases. The barrier to ring closure is only ~14.8 kcal mol^{-1}; however, because of the high number of reactant rotamers involved (162 reactant conformers and 9 TS structures), the probability of assuming the proper substituent orientations for ring closure is reduced, and the predicted ring-closure rate, $k(T) = 1.36 \times 10^{10} \exp(-14.1 \text{ kcal mol}^{-1}/RT)$ s^{-1}, becomes $k_{ringclose} \approx 0.6$ s^{-1} at 298 K. This is still faster than the traditional NO reaction at moderate pollution levels of 1 ppbv of NO. Peroxy ring closure will therefore dominate under most atmospheric conditions.

V. Oxy Ring Closure in Monoterpenes

At elevated NO concentrations, such as in most laboratory experiments, organic peroxy radicals mainly react with NO, forming unsaturated RO• oxy radicals (Scheme 1). For the unsaturated structures considered above, the resulting RO• may likewise undergo ring closure, forming cyclic ether structures. As an example, we examine the oxy radicals formed from α- and β-pinene after the opening of the four-membered ring and subsequent reactions with O_2 and NO (Scheme 4). The oxy radical site can attack the double bond, leading to a cyclic ether radical that will in turn react quickly with O_2 to a cycloether peroxy radical. The importance of this type of reactions is difficult to assess a priori because the rates of the traditional oxy-radical reactions (Scheme 1) depend very strongly on the oxy structure, varying over 10 orders of magnitude.[33] Which reaction dominates is therefore very specific to the compound considered.

In the case of β-pinene, the oxy radical forms five- or six-membered ether rings, assisted by a new H bond with the OH group, which depresses the B3LYP-DFT ring-closure barriers to 1.5 and 3.1 kcal mol^{-1}, respectively. The relative ordering of these TSs, with five-membered ring formation favored over six-membered ring formation, is perhaps unexpected but can

SCHEME 4: Reactions of Oxy Radicals Formed from α-Pinene[a]

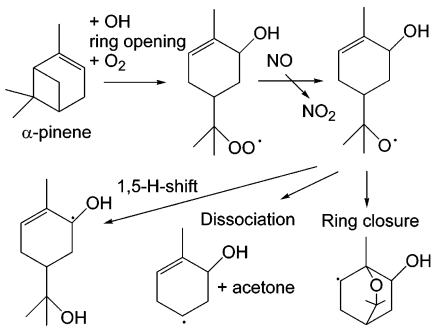

[a] The oxy radicals formed from β-pinene differ only in the position of the −OH substituent.

be readily explained qualitatively by examining the ring strain in the bicyclic structures formed. In the six-membered ether structure, one can visualize three overlapping but distinct six-membered rings; these are all in the boat conformation with an energy[34] of about 6.9 kcal mol^{-1} about the strain-free chair conformation, for a total of 20.7 kcal mol^{-1}. For the compound with the five-membered ether ring, we visualize one five-membered ring, with 6.6 kcal mol^{-1} of ring strain,[34] and two seven-membered rings, with 6.5 kcal mol^{-1} of ring strain each,[34] for a total ring strain of 19.6 kcal mol^{-1}. Hence, in these two bicyclic ether structures one expects similar ring strain, though it is obvious that in similar unicylic structures the six-membered ring will be formed in the chair formation and will therefore be favored over five-membered ring formation. Additional factors in favor of the five-membered ring formation in the β-pinene-derived oxy radical are the higher stability of the tertiary alkyl radical compared to that of a secondary radical and the slightly more favorable H bonding. The low absolute energy barriers of the ring-closure reactions, despite the ring strain, in turn are due to the significant exoergicity of the reaction combined with the fact that ring strain is not yet fully present in the TS and the added bonus of a newly formed strong H bond with the $-CH_2OH$ substituent group. Given the low barriers to ring closure, even when accounting for a possible underestimation of the barrier height (see Methodology), both of these reactions are still energetically favored compared to acetone elimination as well as the 1,5-H shift of the α-hydrogens from the alcohol function to the oxy site,[15] with barriers of 7.5 and 7.1 kcal mol^{-1}, respectively. Ring closure will therefore be the dominant fate.

In oxy radicals formed from α-pinene (Scheme 4) with a syn-positioned OH group (i.e., influenced by H bonding between the oxy radical and the OH substituent), the barrier to acetone elimination (5.2 kcal mol^{-1}) is similar or even slightly lower compared to those for oxy ring closure (5.0 and 6.2 kcal mol^{-1} for six- and five-membered cyclic ethers, respectively). Because the ring-closure TS is also more rigid and therefore entropically disfavored, oxy radical ring closure will barely affect acetone formation from these structures. With the OH group in the anti position, however, the barrier height to dissociation is higher (7.4 kcal mol^{-1}), and the two lowest transition states are those for a 1,5-H shift[15] (~2.7 kcal mol^{-1}) and the oxy ring closure (~4 kcal mol^{-1}). Here, ring closure might alter the reaction products predicted in an earlier theoretical study.[15]

VI. Atmospheric Implications

The full atmospheric degradation mechanisms of the compounds discussed in this paper are much too complex to discuss in full detail here. (See, for example, our degradation mecha-

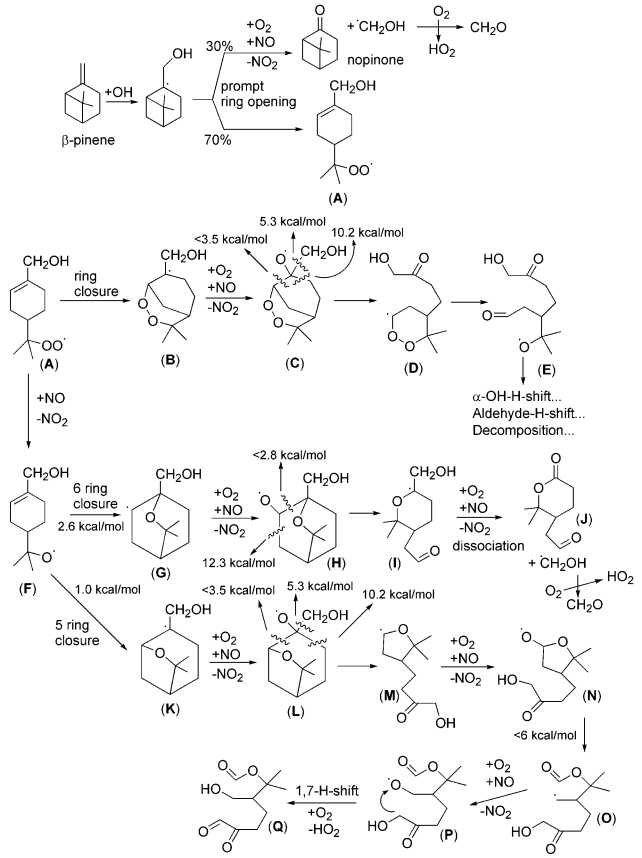

Figure 2. Tentative simplified degradation mechanism of β-pinene following the addition of an OH radical. See the text for a discussion.

nisms for α-pinene[15] and pinonaldehyde[35] or the very extensive literature on isoprene.) Still, it is instructive to discuss at least one example in more detail to place the ring-closure reactions discussed above in their proper perspective. For this purpose, we will examine the OH-initiated oxidation of β-pinene. Compared to α-pinene, for which nearly 100% of the degradation products and their formation mechanism are known (e.g., ref 15), less than 50% of the oxidation products of β-pinene have been quantified to date.[36] Considering the similarity between these two terpenes, this raises serious questions as to the applicability, for β-pinene, of the traditional oxidation pathways that have guided the past laboratory product studies. Here we will show that the apparent anomalous behavior of β-pinene can be rationalized by the (per)oxy ring-closure reactions put forward in this work. However, because a detailed quantum chemical and theoretical kinetic analysis of the complete β-pinene oxidation is far beyond the scope of the present paper, we will present here a tentative mechanism that incorporates the theoretically quantified ring closures but addresses only the first steps of the subsequent chemistry only as far as these can be derived from validated structure−activity relationships (SARs) for alkoxy radical reactions[16,33] and from relevant, specific knowledge gained in our earlier work on the detailed oxidation mechanisms of α-pinene[15] and pinonaldehyde[35] This incomplete, tentative mechanism, depicted in Figure 2, cannot be used for quantitative product yield predictions and is open to (substantial) revisions in a future in-depth investigation.

For this tentative mechanism, we extended our alkoxy radical decomposition SAR[33] by assuming that −OR and −OOR substituents lower the dissociation barrier by an amount that is similar to that of an −OH substituent; this approximation is based on the results of current quantum chemical calculations that will be included in a future extension of the SAR. In the tentative mechanism of Figure 2, the formation of nitrates in peroxy + NO reactions are not included. Neither do we include bimolecular reactions with HO_2 or $R'O_2$ because these induce a branching in the overall mechanism that is beyond the scope of this work.

The dominant initial reaction in the OH-initiated atmospheric oxidation of β-pinene is the addition of OH to the exocyclic carbon of the double bond (≥90%),[15,28,37,38] forming a chemically activated β-hydroxy radical. For the analogous reaction for α-pinene,[15,31] RRKM master equation analyses showed that about 50% of these activated adducts undergo a prompt four-membered ring opening with a barrier of about 12 kcal mol^{-1}. In β-pinene, the calculated barrier to ring opening is slightly lower, 10.5 kcal mol^{-1}, so a somewhat higher prompt ring-opening yield is expected, leading to a hydroxyl-menthenyl radical that will react rapidly with O_2, forming a hydroxymenthenylperoxy radical (**A**); see Figure 2. The remaining fraction of the initial OH adduct will react with O_2, form an oxy radical after reaction with NO, and dissociate into nopinone + $^{\bullet}CH_2$-OH. Nopinone has been observed experimentally with a total overall yield of about 27%.[36] This implies a ratio of ring-opening versus thermalisation of about 70:30 for the initial OH adduct, which is in agreement with the theoretical expectations.

The HO-menthenylperoxy radical (**A**) ring closure can outrun the reaction with NO at low-to-moderate NO concentrations ≤1 ppbv (see above), yielding a bicyclic compound (**B**) that will in turn rapidly react with O_2. The peroxy radical thus formed is then converted to an oxy radical (**C**) by reaction with NO. The bicyclic oxy radical (**C**) can dissociate in three ways: with SAR[33] barriers of 10.2, 5.3, and 3.5 kcal mol^{-1}, where this last value should be lowered further by the release of ring strain. This last dissociation is therefore expected to dominate, with the formation of a cyclic α-(alkylperoxy)-alkyl radical featuring an exocyclic β-hydroxy-ketone functionality (**D**). CCSD(T)//B3LYP-DFT calculations[39] show that α-(alkylperoxy)-substituted radicals dissociate on a (sub)picosecond time scale into a carbonyl and an oxy radical. For the cyclic radical (**D**), this implies ring opening to form an oxy radical (**E**). The subsequent degradation of **E** cannot be easily predicted because it involves competition between fast alkoxy decomposition, in casu acetone elimination versus a quasi-barrierless[15] H shift from the aldehyde group, or a H shift from the α-hydroxy-β-carbonyl site that is also expected to have a low barrier. From this point onward, the mechanism can branch strongly, and detailed theoretical kinetic analyses are therefore required to determine the subsequent chemistry.

Under high-NO conditions such as in laboratory experiments, the initial HO-menthenylperoxy radical (**A**) will convert to a hydroxymenthenoxy radical (**F**), for which ring-closure barriers were calculated to be 3.1 kcal mol^{-1} (→ six-ring ether) and 1.5 kcal mol^{-1} (→ five-ring ether). These two ring closures will certainly outrun all other potential reactions, though it is currently not possible to quantify the relative contributions of five- versus six-membered ring formation. The six-membered cyclic ether radical (**G**) will react with O_2 and NO to form a cyclic alkoxy radical (**H**), which can dissociate in two ways. The SAR barriers[33] for these two channels are 12.3 (negligible contribution) and 2.8 kcal mol^{-1}, with the latter expected to be lowered further by ring-strain relaxation. The dominant β-hydroxy product (**I**) reacts with O_2 and NO to form a β-hydroxy alkoxy radical that subsequently dissociates into $^{\bullet}CH_2OH$ and the substituted cyclic ester (**J**). However, the five-membered cyclic ether radical (**K**) will form a β-OH-β'-ether alkoxy radical

(**L**) by reaction with O_2 and NO. The SAR barriers[33] for the dissociation of **L** are 10.2, 5.3, and 3.5 kcal mol^{-1}. Because the lowest barrier needs to be adjusted downward to account for the reduction in ring strain, one expects the prevalent formation of the cyclic ether radical (**M**), which will be converted to a β-ether alkoxy radical (**N**) by reaction with O_2 and NO. With a SAR decomposition barrier of only 6 kcal mol^{-1},[33] lowered even further by the release of ring strain in the five-membered ring, this alkoxy radical will undergo ring breaking, forming a formate ester (**O**). The radical site will subsequently react with O_2 and NO, forming a primary alkoxy radical (**P**). The dissociation of **P** to eliminate CH_2O faces a rather high SAR barrier of 11 kcal mol^{-1} and is most likely outrun by a 1,7-H shift from the α-hydroxy-β-keto site with a barrier of $\leq$6 kcal mol^{-1},[15] followed by hydrogen abstraction by O_2, leading finally to the hydroxyl-diketone formate (**Q**).

The preliminary mechanism described above and depicted in Figure 2 can aim to capture only the main features of the atmospheric oxidation of β-pinene and must await experimental and more detailed theoretical confirmation. Nevertheless, given the large fraction of the dominant primary OH adduct undergoing prompt four-membered ring opening, a substantial fraction of the reaction flux should pass through intermediates that will mainly react by (per)oxy ring closures (i.e., HO-menthenyl-peroxy radicals under low-NO conditions and HO-menthenoxy radicals under high-NO conditions). In all reaction pathways, the formation of oxygenates with multiple oxygen-bearing functionalities is found.

Finally, it is interesting to contrast the present findings with a mechanism in which (per)oxy ring-closure reactions are not considered. With an estimated 90% of OH addition occurring on the outer carbon of the double bond, 70% subsequent prompt ring opening, sufficient NO to convert peroxyradical **A** to OH menthenoxyradical **F** and accounting for about 11% of the nitrate formation in the NO reaction,[40] 56% of the reaction flux is predicted to pass through oxy radical **F**. In the absence of ring-closure reactions, the dominant reaction pathway for this oxy radical is dissociation to form acetone, with a calculated barrier of 7.0 kcal mol^{-1}. A potential competing reaction (i.e., a 1,5-H shift to form an allyl resonance-stabilized radical) has a calculated barrier of 6.6 kcal mol^{-1}, but the very small energetic advantage for this channel is outdone by the loss of the $-C(CH_3)_2O^{\bullet}$ and $-CH_2OH$ internal rotations. This latter group forms a H bond with the oxy radical, lowering the 1,5-H shift TS from the calculated value of 8.0 kcal mol^{-1} without H-bond assistance. Hence, a 1,5-H shift is strongly disfavored entropically. Likewise, a 1,4-H-shift forming the alternative allyl resonance-stabilized radical is disfavored both entropically and energetically. A 1,7-H shift from the α-OH site is geometrically impossible because of the planar geometry near the double bond causing the $-CH_2OH$ hydrogens to be too far from the oxy radical site. Hence, with the loss of acetone as the main predicted fate of alkoxy radical **F**, one finds a yield of >50% acetone. This blatantly contradicts the experimental product measurements, where an average acetone yield of only 7.5% is found, with the highest reported value being 13%.[36] From this, we conclude that nontraditional reaction pathways (i.e., the proposed ring-closure reactions) are required to explain the experimental product measurements.

The mechanism presented in Figure 2 can serve as a guide to experimental work; in particular, the formation of cyclic esters/ethers and formates under high-NO reaction conditions are worth investigating.

VII. Conclusions

We have shown that hitherto neglected "exotic" ring-closure reactions in unsaturated peroxy- and oxy radicals are expected to be important pathways in the atmospheric chemistry of the most abundant nonmethane VOCs. Peroxy ring closure is enhanced by increasing substitution and is also facilitated by intramolecular H bonding. After comparing with the rate coefficients of traditional peroxy-radical removal reactions, we have shown that ring closure is a major channel not only in remote regions but also for some $ROO^{\bullet}$, even in areas with increased NO levels. Rearrangement to epoxide-oxy structures after peroxy ring closure was found not to be competitive, in contrast to the equivalent bimolecular reactions of peroxy radicals with olefins. Whether the peroxide ring is preserved in the final degradation products depends on the specific structure of the VOC studied, but if retained, these highly oxygenated and therefore low-volatility peroxy ring products will likely contribute to SOA.

The impact of ring closure in unsaturated oxy radicals can be determined only by examining the full degradation mechanism of the pertaining organic compound because the fate of oxy radicals depends strongly on their specific structure. For monoterpenes α-pinene and β-pinene, we compared the barrier heights for oxy radical ring closure to those of the other competing unimolecular reactions. In some cases, ring closure is predicted to have a negligible effect, whereas in other cases, the calculations indicate that ring closure is the dominant channel.

The full degradation mechanisms of the VOCs discussed in this paper are very complex, and the ultimate impact of ring-closure reactions on the final products can be examined only on a case-by-case basis. For the most important compounds at issue, the full degradation mechanisms will be investigated in detail in separate publications. A preliminary OH-initiated oxidation mechanism for β-pinene is presented, showing the crucial importance of (per)oxy ring-closure reactions. It is also shown that the nontraditional ring-closure reaction pathways proposed here are required to bring the theoretical predictions into agreement with the experimental yields of traditional-pathway products. Our present contribution also aims to stimulate experimental work targeting the likely products of ring-closure reactions to confirm and quantify their contribution under atmospheric reaction conditions.

Acknowledgment. We thank the Belgian Federal PFOW office, the European Commission, the Fund for Scientific Research Flanders (FWO-Vlaanderen), and the K.U. Leuven Research Council (BOF Fund and GOA) for continuing support. L.V. is a postdoctoral fellow of the FWO-Vlaanderen.

Supporting Information Available: Absolute energies, zero-point energies, vibrational frequencies, Cartesian coordinates for species and transition states investigated in this work. This material is available free of charge via the Internet at http://pubs.acs.org. It is also available directly from the authors' website at http://arrhenius.chem.kuleuven.ac.be/labpeeters.

References and Notes

(1) Guenther, A.; Hewitt, C. N.; Erickson, D.; Fall, R.; Geron, C.; Graedel, T.; Harley, P.; Klinger, L.; Lerdau, M.; McKay, W. A.; Pierce, T.; Scholes, B.; Steinbrecher, R.; Tallamraju; R.; Taylor, J.; Zimmerman, P. *J. Geophys. Res.* **1995**, *100*, 8873.

(2) Roelofs, G.-J.; Lelieveld, J. *J. Geophys. Res.* **2000**, *105*, 22697.

(3) Wang, Y.; Jacob, D. J.; Logan, J. A. *J. Geophys. Res.* **1998**, *103*, 10757.

(4) Andreae, M. O.; Crutzen, P. J. *Science* **1997**, *276*, 1052.
(5) A*tmospheric Chemistry in a Changing World*; Brasseur, G. P., Prinn, R. G., Pszenny, A. A. P., Eds.; Springer-Verlag: Berlin, 2003.
(6) Paulson, S. E.; Seinfeld, J. H. *J. Geophys. Res.* **1992**, *97*, 20703.
(7) Zhang, D.; Zhang, R.; Park, J.; North, S. W. *J. Am. Chem. Soc.* **2002**, *124*, 9600.
(8) Kwok, E. S.; Atkinson, R.; Arey, J. *Environ. Sci. Technol.* **1995**, *29*, 2467.
(9) Wisthaler, A.; Jensen, R.; Winterhalter, R.; Lindinger, W.; Hjorth, J. *Atmos. Environ.* **2001**, *35*, 6181.
(10) Orlando, J. J.; Nozière, B.; Tyndall, G.; Orzechowska, G. E.; Paulson, S. E.; Rudich, Y. *J. Geophys. Res.* **2000**, *105*, 11561.
(11) Benkelberg, H.-J.; Böge, O.; Seuwen, R.; Warneck, P. *Phys. Chem. Chem. Phys.* **2000**, *2*, 4029.
(12) Nozière, B.; Barnes, I.; Becker, K. H. *J. Geophys. Res.* **1999**, *104*, 23645.
(13) Ruppert, L.; Becker, K.-H. *Atmos. Environ.* **2000**, *34*, 1529.
(14) Miyoshi, A.; Hatakeyama, S.; Washida, N. *J. Geophys. Res.* **1994**, *99*, 18779.
(15) Peeters, J.; Vereecken, L.; Fantechi, G. *Phys. Chem. Chem. Phys.* **2001**, *3*, 5489.
(16) Atkinson, R. *J. Phys. Chem. Ref. Data.* **1997**, *26*, 215.
(17) Vereecken, L.; Peeters, J. *J. Chem. Phys.* **2003**, *119*, 5159.
(18) Becke, A. D. *J. Chem. Phys.* **1993**, *98*, 5648.
(19) Lee, C.; Yang, W.; Parr, R. G. *Phys. Rev. B* **1988**, *37*, 785.
(20) Atkinson, R.; Carter, W. P. L.; Darnall, K. R.; Winer, A. M.; Pitts, J. N. *Int. J. Chem. Kinet.* **1980**, *12*, 779.
(21) Lay, T. H.; Bozzelli, J. W.; Seinfeld, J. H. *J. Phys. Chem.* **1996**, *100*, 6543.
(22) Motta, F.; Ghigo, G.; Tonachini, G. *J. Phys. Chem. A* **2002**, *106*, 4411.
(23) Stark, M. S. *J. Phys. Chem.* **1997**, *101*, 8296 and references therein.
(24) Brasseur, G. P.; Hauglustaine, D. A.; Walters, S.; Rasch, P. J.; Muller, J.-F.; Granier, C.; Tie, X. X. *J. Geophys. Res.* **1998**, *103*, 28265.
(25) Finlayson-Pitts, B. J.; Pitts, J. N., Jr. *Chemistry of the Upper and Lower Atmosphere*; Academic Press: San Diego, CA, 2000.
(26) Frisch, M. J.; Trucks, G. W.; Schlegel, H. B.; Scuseria, G. E.; Robb, M. A.; Cheeseman, J. R.; Zakrzewski, V. G.; Montgomery, J. A., Jr.; Stratmann, R. E.; Burant, J. C.; Dapprich, S.; Millam, J. M.; Daniels, A. D.; Kudin, K. N.; Strain, M. C.; Farkas, O.; Tomasi, J.; Barone, V.; Cossi, M.; Cammi, R.; Mennucci, B.; Pomelli, C.; Adamo, C.; Clifford, S.; Ochterski, J.; Petersson, G. A.; Ayala, P. Y.; Cui, Q.; Morokuma, K.; Malick, D. K.; Rabuck, A. D.; Raghavachari, K.; Foresman, J. B.; Cioslowski, J.; Ortiz, J. V.; Stefanov, B. B.; Liu, G.; Liashenko, A.; Piskorz, P.; Komaromi, I.; Gomperts, R.; Martin, R. L.; Fox, D. J.; Keith, T.; Al-Laham, M. A.; Peng, C. Y.; Nanayakkara, A.; Gonzalez, C.; Challacombe, M.; Gill, P. M. W.; Johnson, B. G.; Chen, W.; Wong, M. W.; Andres, J. L.; Head-Gordon, M.; Replogle, E. S.; Pople, J. A. *Gaussian 98*, revision A.9; Gaussian, Inc.: Pittsburgh, PA, 1998.
(27) Jenkin, M. E.; Boyd, A. A.; Lesclaux, R. *J. Atmos. Chem.* **1998**, *29*, 267.
(28) Peeters, J.; Boullart, W.; Pultau, V.; Vandenberk, S. In *Proceedings of EUROTRAC Symposium '96*; Borrell, P. M., et al., Eds.; Computational Mechanics Publications: 1996; pp 471−475.
(29) McGivern, W. S.; Suh, I.; Clinkenbeard, A. D.; Zhang, R. Y.; North, S. W. *J. Phys. Chem. A* **2000**, *104*, 6609.
(30) Park, J.; Jongsma, C. G.; Zhang, R. Y.; North, S. W. *Phys. Chem. Chem. Phys.* **2003**, *5*, 3638.
(31) Vereecken, L.; Peeters, J. *J. Phys. Chem. A* **2000**, *104*, 11140.
(32) Singh, H. B.; Kanakidou, M.; Crutzen, P. J.; Jacob, D. J. *Nature* **1995**, *378*, 50.
(33) Peeters, J.; Fantechi, G.; Vereecken, L. *J. Atmos. Chem.*, in press, 2004.
(34) Pedley, J. B. *Thermochemical Data and Structures of Organic Compounds*; TRC Data Series; Thermodynamics Research Center: College Station, TX, 1994; Vol. 1.
(35) Fantechi, G.; Vereecken, L.; Peeters, J. *Phys. Chem. Chem. Phys.* **2002**, *4*, 5795.
(36) Atkinson, R.; Arey, J. *Atmos. Environ.* **2003**, *37*(supplement 2), 197.
(37) Kwok, E. S. C.; Atkinson, R. *Atmos. Environ.* **1995**, *29*, 1685.
(38) Vereecken, L.; Peeters, J. *Phys. Chem. Chem. Phys.* **2002**, *4*, 467.
(39) Vereecken, L.; Nguyen, T. L.; Peeters, J. submitted, 2004.
(40) Arey, J.; Aschmann, S. M.; Kwok, E. S. C.; Atkinson, R. *J. Phys. Chem A* **2001**, *105*, 1020.